



**SINTEF**

# **Report**

**Final report: Climit project 616067  
"Accurate CO2 monitoring using  
quantitative joint inversion for  
large-scale on-shore and off-shore  
storage applications" (aCQurate)  
October 2022**

**Client(s):**

Gassnova/CLIMIT



SINTEF

SINTEF Industry  
Postal address:  
Postboks 4763 Torgarden  
7465 Trondheim

Switchboard: +47 40005100  
info@sintef.no

Enterprise /VAT No:  
NO 919 303 808 MVA

# Report

## Final report: Climit project 616067 "Accurate CO2 monitoring using quantitative joint inversion for large-scale

### KEYWORDS

CO2 monitoring, joint inversion,  
structural inversion, petrophysical  
inversion, Ketzin pilot site

### VERSION

1.1

### DATE

2022-11-04

### AUTHOR(S)

Michael Jordan

### CLIENT(S)

Gassnova/CLIMIT

### CLIENT'S REFERENCE

Klikk eller trykk her for å skrive  
inn tekst.

### PROJECT NO.

102017306

### NO. OF PAGES/APPENDICES

27

### SUMMARY

The SINTEF coordinated aCQurate project (2016-2022) aimed to develop a method to allow quantitative estimation of key reservoir parameters (e.g., saturation, pressure, stress, or strain in the overburden) for the monitoring of CO<sub>2</sub> storage sites. This was achieved by integrating methods relevant for CO<sub>2</sub> storage through an advanced hybrid structural-petrophysical joint inversion method and by demonstrating its capabilities using data from the Field Research Station (CaMI.FRS) and from the Ketzin site in Germany. This project was conducted in collaboration with partners from Canada, the US, Germany and Norway.

### PREPARED BY

Michael Jordan

SIGNATURE

### CHECKED BY

Bastien Dupuy

SIGNATURE

### APPROVED BY

Peder Eliasson

SIGNATURE

COMPANY WITH  
MANAGEMENT SYSTEM  
CERTIFIED BY DNV  
ISO 9001 • ISO 14001  
ISO 45001

### REPORT NO.

[Klikk eller trykk  
her for å skrive

### ISBN

Klikk eller trykk her  
for å skrive inn

### CLASSIFICATION

Internal

### CLASSIFICATION THIS PAGE

Internal

# Document history

---

VERSION	DATE	VERSION DESCRIPTION
[versjon]	Klikk eller trykk her for å velge dato	[Tekst]

---

# Table of contents

<b>1</b>	<b>Final project summary</b> .....	<b>4</b>
<b>2</b>	<b>Summary of results</b> .....	<b>6</b>
2.1	From well to data .....	6
2.2	Joint Inversion developments .....	7
2.2.1	General description of the joint inversion.....	7
2.2.2	Implementation .....	8
2.2.3	Workflow .....	9
2.3	Application to synthetic and real FRS data .....	10
2.3.1	Joint inversion application to synthetic FWI and ERT data from CaMI.FRS .....	10
2.3.2	Joint inversion application to real FWI and ERT data from the Ketzin pilot site, Germany .....	12
2.3.3	Application to cross-well seismic and downhole ERT data from CaMI.FRS .....	14
2.3.4	Application to VSP seismic and downhole ERT data from CaMI.FRS .....	16
2.4	Petrophysical quantification and interpretation .....	18
2.5	Tilt measurements and derivation of strain .....	20
<b>3</b>	<b>Meetings, reports, presentations, and publications</b> .....	<b>23</b>
<b>4</b>	<b>Project implementation and resource use</b> .....	<b>26</b>
<b>5</b>	<b>References</b> .....	<b>27</b>

## APPENDICES

Klikk eller trykk her for å skrive inn tekst.

## 1 Final project summary

The aim of the aCQurate project was to develop a method for quantitative estimation of key reservoir parameters (e.g., saturation, pressure, stress, or strain in the overburden) for the monitoring of CO<sub>2</sub> storage sites. This was achieved by integrating methods relevant for CO<sub>2</sub> storage through an advanced hybrid structural-petrophysical joint inversion method and by demonstrating its capabilities using data from the Field Research Station (CaMI.FRS). Data from the CaMI.FRS and Ketzin test sites were also instrumental for testing and maturation of the method for application to larger-scale sites. In addition, a second goal of the project was to share and distribute knowledge within the field through the collaboration with experts in Canada and the US.

Quantification of reservoir parameters is often done in a two-stage approach: in a first stage, geophysical data are processed and inverted to obtain models of the distribution of geophysical parameters (e.g., seismic velocity, resistivity, or density) in the underground. In a second stage, these models are used as input in a rock physics inversion to derive quantitative estimates of reservoir parameters, such as the saturation of CO<sub>2</sub> and pore pressure). As the outcome of the rock physics inversion directly depends on the provided geophysical models, this project focuses on the first step, i.e., the geophysical input models. In addition, to reduce the uncertainties in the rock-physics inversion results, using more than one geophysical model (e.g., seismic velocities and resistivities) is beneficial.

Therefore, the objective of this project was to develop a new method for monitoring injected CO<sub>2</sub> using a hybrid structural-petrophysical joint inversion approach. The aim of this development was to provide a method for accurate and reliable CO<sub>2</sub> monitoring for large-scale onshore and offshore storage applications. The joint inversion combines the strengths and advantages of different geophysical monitoring techniques. The hybrid approach integrates the robustness of the structural joint inversion with the inherent quantitative calibration of the petrophysical joint inversion. The resulting models are consistent with each other, with all data sets and constraints, and with any prior information.

To address the stress and strain in the overburden, additional surface deformation measurements, e.g., using tilt meters, could be used. The observed surface deformation can be related to the reservoir pressure, stress and strain in the overburden using geomechanical modelling. This can be integrated with the joint inversion results and provide additional input to the rock physics inversion. While including these measurements in the analysis was not part of this project, it was considered as potential second phase or add-on project. As part of this project a feasibility study was conducted to investigate if such measurements could be conducted at CaMI.FRS.

As the resulting method was intended to be applicable to real sites on the Norwegian Continental Shelf (NCS), the joint inversion was designed for large-scale data while at the same time allowing high resolution imaging of the target area. In addition, it should be applicable to onshore and offshore settings and allowing quantitative evaluation of the results. The large-scale and high-resolution requirement was achieved using a combination of 1) the implementation of the joint inversion software on HPC infrastructure, and 2) by focusing the joint inversion on a target area. The applicability to onshore and offshore settings was realized by including the relevant methods for each case. Relevant methods for onshore applications are: seismic full waveform inversion (FWI), electrical resistivity tomography (ERT), gravity (SINTEF in-house), and magnetometric resistivity (MMR). Corresponding methods for offshore applications are FWI, controlled source electromagnetics (CSEM), and gravity. The implementation was designed to be flexible and modular, so that the joint inversion code can be used with the geophysical methods that are best suited to a particular application. In addition to the methods mentioned in the project proposal, we integrated a second CSEM

method (Mare2DEM, Key(2016)), and a SINTEF ray-based seismic tomography code for seismic cross-well and VSP (Vertical Seismic Profiling) inversions.

The project was conducted in tight collaboration with Canadian, US, and German project partners throughout the project. The international collaboration was extended to also include Columbia University, USA. Several visits and international meetings were arranged during the duration of the project, including a one-month visit of a PhD student from the University of Calgary to SINTEF, and several visits of the project's postdoc to Canada to conduct measurements at the CaMI site.

Project results were summarized in nine different deliverables (L1-L9):

Deliverable L1 contained a tilt meter feasibility study investigating the sensitivity of surface deformation and tilt measurements at CaMI.FRS to expected pressure changes in the reservoir. Deliverables L2 and L3 provided an overview of available baseline and repeat measurements, data processing, and existing models for the different geophysical monitoring techniques that may be relevant for the joint inversion conducted in the aCQurate project. Deliverable L4 consisted of a report assessing and evaluating alternative and new methods for CO<sub>2</sub> monitoring that may become relevant for quantification of key reservoir parameters and/or use as part of a joint inversion in the future. Deliverables L5, L6a, and L6b reported on the different stages of the joint inversion method and software development. L5 consisted of a report focusing on the code structure and implementation to ensure that the resulting software would be capable of handling high-resolution/large-scale applications. L6a consisted of a report summarizing the status of the joint inversion software and associated workflow. The report also provided examples of the application to synthetic FWI and ERT data based on the CaMI.FRS site. L6b consisted of a manuscript for publication, where the hybrid joint inversion was applied and demonstrated using real field data (FWI and ERT) from the Ketzin pilot site in Germany. Deliverables L7 and L8 also consisted of manuscripts for publication of the application of the joint inversion code to seismic cross-well and downhole ERT data (L7) and VSP seismic and downhole ERT data (L8). Deliverable L9 was a report describing the application of the quantification step to results from the joint seismic cross-well and downhole ERT data from L7.

**Project leader:**

SINTEF

**Gassnova contact person:**

Kari-Lise Rørvik, Gassnova, [klr@gassnova.no](mailto:klr@gassnova.no)

**Research Partners:**

- CMC Research Institutes, Containment and Monitoring Institute (CaMI), Calgary, Canada
- University of Calgary, Calgary, Canada
- Institut national de la recherche scientifique (INRS), Québec, Canada
- Lawrence Berkeley National Laboratory, Energy Geosciences Division, Berkeley (LBNL), USA
- Scripps Institution of Oceanography, University of California, San Diego, USA
- GFZ German Research Centre for Geosciences, Potsdam, Germany

**Industry partners:**

- Equinor
- Quad Geometrics

## 2 Summary of results

The project was organized in five different work packages. Each of these work packages contributed to the common goal and outcome to develop a new hybrid joint inversion technology for accurate CO<sub>2</sub> monitoring for large-scale on-shore and off-shore storage applications.

### 2.1 From well to data

Work package 1 consisted of the contributions of the Canadian partners (CaMI, University of Calgary, and INRS) that consisted of the injection of CO<sub>2</sub> at 300 m depth and data acquisition for seismic, ERT, electromagnetic, and magnetometric data. This was fundamental to obtain the necessary 4D data for the development, testing, and demonstration of the joint inversion. In addition, this work package also included the data processing and analysis of these data types, as well as the preparation of the models and data for joint inversion (CaMI, UCalgary, LBNL, INRS, and GFZ/SINTEF).

This effort is documented in deliverables L2 and L3 but contributed to all deliverables.

Figure 1 provides a map indicating the layout of the CaMI.FRS site, including the location of the wells and the surface facilities. Figure 2 shows the CO<sub>2</sub> injection history until 2021.

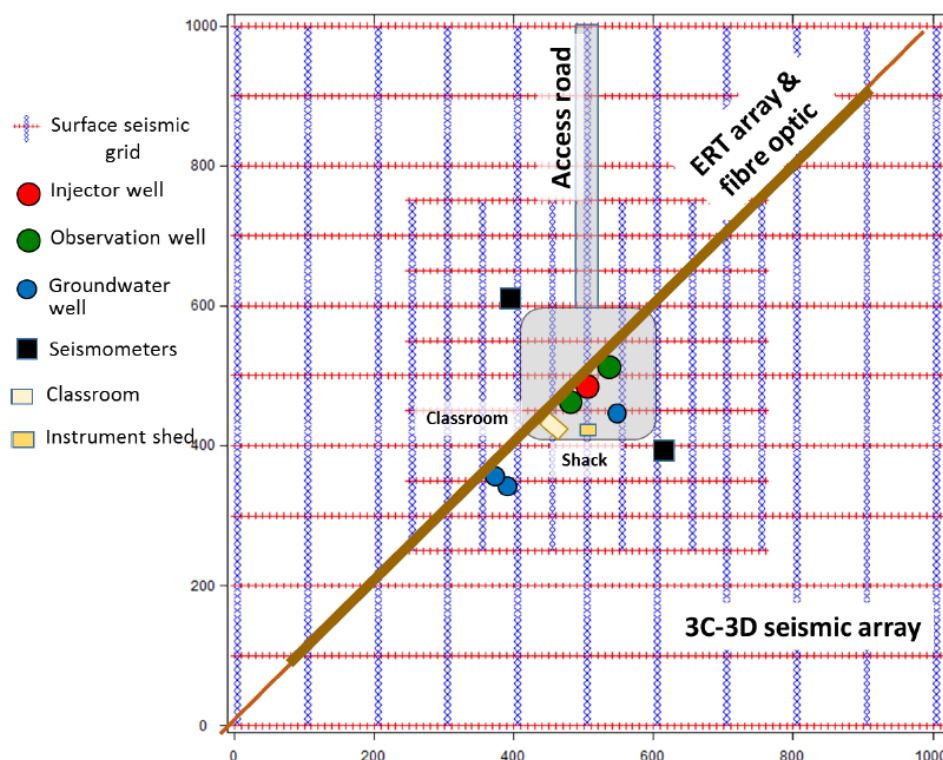


**Figure 1:** Map of the CO<sub>2</sub> injection facilities and monitoring layout at CaMI.FRS.

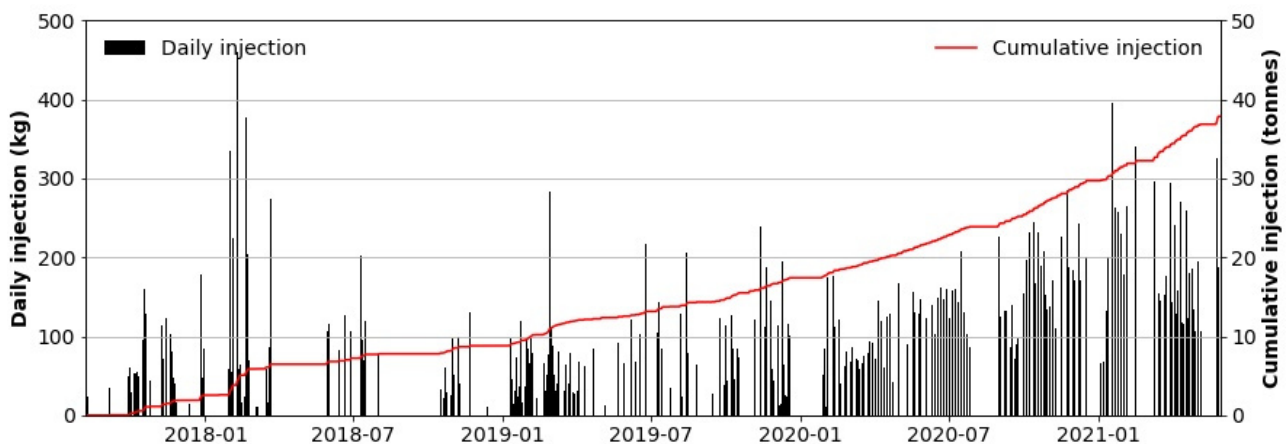


**Figure 2:** Injection history at CaMI.FRS.

Seismic data acquisition included seismic surveys recorded by surface geophones, seismic surveys recorded by DAS cables, regular walk-away and walk around VSP surveys. Electro-magnetic monitoring included EM-surveys, MMR, and ERT surveys. In particular, the VSP and ERT surveys, and corresponding data processing, analysis and interpretation was very valuable for the aCQurate project as this allowed a close follow up on the status and detectability of the injected CO<sub>2</sub>. In addition, the VSP, cross-well seismic, and ERT data were used as input for the joint inversion.

## 2.2 Joint Inversion developments

The joint inversion developments were documented in detail in deliverables L5, L6a, and L6b.

### 2.2.1 General description of the joint inversion

We developed a novel hybrid joint inversion methodology for onshore and off-shore CO<sub>2</sub> storage applications. It integrates multiple geophysical monitoring techniques and has been designed for large-scale applications and high-resolution monitoring. In the context of CO<sub>2</sub> monitoring, where strong emphasis is on the ability to perform quantitative monitoring of pressure and saturation, this is generally done in a two-step approach. In a first step, geophysical models of the reservoir and subsurface are derived, which in a second step are inverted together to derive rock physics parameters. The joint inversion methodology aims to provide the best possible geophysical models of the reservoir and subsurface, which are a prerequisite for achieving accurate quantitative estimates of saturation and pressure. Despite the primary focus on CO<sub>2</sub> monitoring, the hybrid joint inversion is not limited to these applications but can also be used in other scenarios combining different geophysical data sets.

The joint inversion combines the strengths and advantages of different geophysical monitoring techniques (e.g., seismics with its high spatial resolution and geoelectrics with its high sensitivity to changes in CO<sub>2</sub> saturation). Our hybrid joint inversion uses a cross-gradient approach to achieve structural similarity between the different models. While this structural joint inversion provides a robust link between models of different geophysical monitoring techniques, it does not use or require a physical relationship between the different model parameter types. Therefore, the structural joint inversion lacks control of the model parameter amplitudes, unless the models are otherwise constrained or calibrated using valid rock-physics models. This limitation is addressed by adding a rock-physics link between the different model parameters, in the form of cross-property relations, e.g., derived from well logs. The general concept of this new hybrid structural-petrophysical joint inversion is illustrated in Figure 3. Unlike the structural joint inversion, which is valid everywhere in the model space, the petrophysical joint inversion is only valid where appropriate rock physics models or cross-property relations are available (e.g., at and around wells).

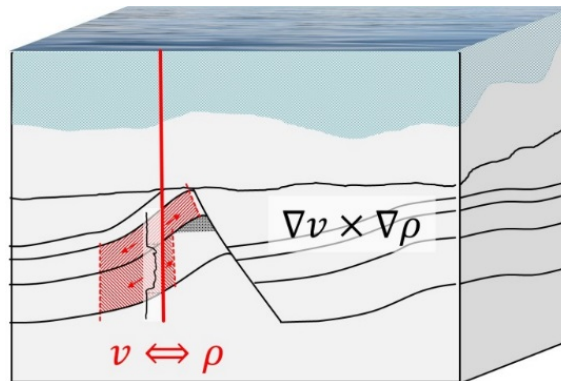


Figure 3: Sketch illustrating the hybrid joint inversion. It consists of a structural and a petrophysical part. While the structural joint inversion (indicated by  $\nabla v \times \nabla \rho$ ) is valid everywhere in the model space, the petrophysical joint inversion is only valid where appropriate rock physics models or cross-property relations are available (e.g., at and around wells).

### 2.2.2 Implementation

The joint inversion is implemented using a Bayesian approach. It allows the incorporation of a priori information in the joint inversion, i.e., both specific knowledge of certain model parameters, as well as information about data accuracy, and the general expected model variations. It is also used for the crucial weighting of the different data types and constraints and their influence on the joint inversion result.

The structural part of the joint inversion uses a cross-gradient constraint to ensure structural similarity (e.g., Gallardo and Meju, 2004; Jordan et al., 2018). It does not require a priori knowledge about the relations between the model parameters and is valid in the whole model space.

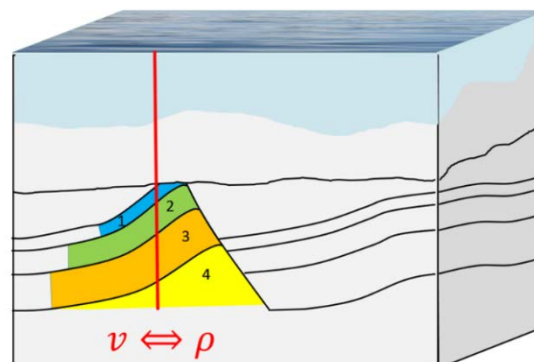


Figure 4: Sketch illustrating the implementation of the petrophysical joint inversion constraint. The subsurface is divided into several petrophysical units (1-4), for which different cross-property relations are defined. The petrophysical joint inversion constraint is only valid where appropriate rock physics models or cross-property relations are available (e.g., at and around wells), but can likely be extended into the surrounding model space by following stratigraphic units.

The links between the geophysical parameters (e.g., velocity, resistivity, and density) are established using cross-property relations derived from rock physics models. In our approach the exact correlation is not considered fully known, but rather represented by a quasi-linear relationship (e.g., Zeyen and Achauer, 1997). The part of the subsurface where the petrophysical relation is applied can be divided into several units (see Figure 4), e.g., following geological boundaries. Each unit is attributed a rock physics relation. To account for their uncertainties, we treat the correlation parameters as additional parameters and include them as additional parameters in the joint inversion.

The actual joint inversion is realized using a quasi-Newton formulation with gradient vector and Hessian matrix. The different constraints of the individual methods (e.g., seismic and ERT) are combined in one single system of equations, which is solved to provide the joint inversion results. These constraints consist of data fit, model constraints, and the structural and petrophysical constraints. While the gradient vector is extended to include the two different methods and the correlation parameters from the rock-physics inversion, the actual coupling of both models (i.e., the joining of the different methods) is established by filling the off-diagonal elements of the Hessian with second partial derivatives from the joint inversion constraints.

The implementation of the different geophysical methods is modular and allows the inclusion of additional third-party geophysical methods. Initially it was planned to include seismic FWI, CSEM, ERT, gravity, and MMR into the joint inversion. However, during the project, ray-based seismic first arrival time tomography, and an additional external CSEM method (Mare2DEM, Key (2016)) was implemented for cross-well and VSP seismic applications described in section 2.3 below.

In addition, emphasis is placed on the computational efficiency. To handle the large inverse problems to be solved, the joint inversion code is implemented in Fortran 90 as a hybrid OpenMP/MPI parallel code. While OpenMP is used for parallelism within a multi-core node, MPI is used for parallelism between nodes. For large-scale and high-resolution applications, efficient implementation of the joint inversion is important. As one means to address these requirements, a target-oriented approach was implemented, where the joint inversion can be restricted to a target zone, e.g., the reservoir where the CO<sub>2</sub> is injected. This allows the reduction of the number of model parameters in the joint inversion, and a significant increase of the spatial resolution in the targeted area.

### 2.2.3 Workflow

The successful application of the joint inversion depends on the correct selection of a large number of weighting parameters. As it is unreasonable and potentially impossible to test all possible parameter combinations and settings, we developed a workflow that can lead the application so that reliable results can be obtained in a reasonable amount of time. The workflow consists of conducting individual inversions, then conducting structural and petrophysical joint inversions independently from each other, and finally to conduct the two joint inversions together.

## 2.3 Application to synthetic and real FRS data

The joint inversion method was applied to synthetic and real data from the CaMI.FRS site as planned, and in addition, due to delays caused by the Corona pandemic, to data from the Ketzin pilot site in Germany.

Main applications included:

- Application to synthetic FWI and ERT data from CaMI.FRS (Deliverable L6a)
- Application to real data from Ketzin pilot site in Germany (Deliverable L6b)
- Application to cross-well seismic and downhole ERT data from CaMI.FRS (Deliverable L7)
- Application to VSP seismic and downhole ERT data from CaMI.FRS (Deliverable L8)

In addition, a joint cross-well seismic and cross-well CSEM inversion was conducted for the baseline case. In the following we will show examples of joint inversion results for the different cases.

### 2.3.1 Joint inversion application to synthetic FWI and ERT data from CaMI.FRS

Synthetic baseline and repeat data representing the CaMI.FRS site were obtained by forward-modelling seismic and ERT data from geostatic synthetic seismic velocity and electrical resistivity models. For the repeat models and data, dynamic fluid flow simulations with 1330 t of CO<sub>2</sub> over 5 years (Macquet et al., 2018) resulted in velocity and resistivity changes due to fluid substitution inferred from Gassmann's Equation and Archie's Law. The corresponding velocity and resistivity models at the well location are shown in Figure 5.

Figure 5 also shows the relation between velocity and resistivity model, which is used to define a three-layer petrophysical (cross-property) model for the petrophysical part of the joint inversion.

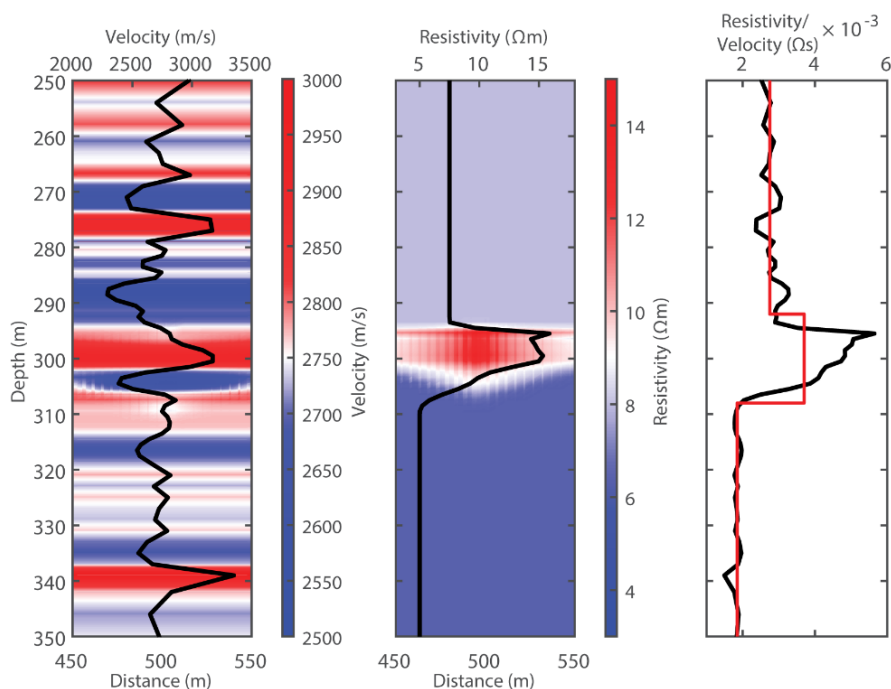


**Figure 5:** "True" velocity- (left) and resistivity (center) structures around the well locations, with synthetic logs (black lines) at the wells. Resistivity-velocity relation (right; black line) and the corresponding 3-layer petrophysical model (B-parameters; red line).

A joint inversion of seismic FWI, using a line of sources and receivers at the surface, and downhole ERT measurements was conducted. Figure 6 shows a comparison of independent and joint inversion results for a case where the petrophysical constraints are only used at the well location.

In the uppermost two rows it shows the "true" synthetic model and the seismic and ERT starting models that were used for all independent and joint inversion results below. Results for the petrophysical, the structural and the hybrid joint inversions are provided in rows 3-5.

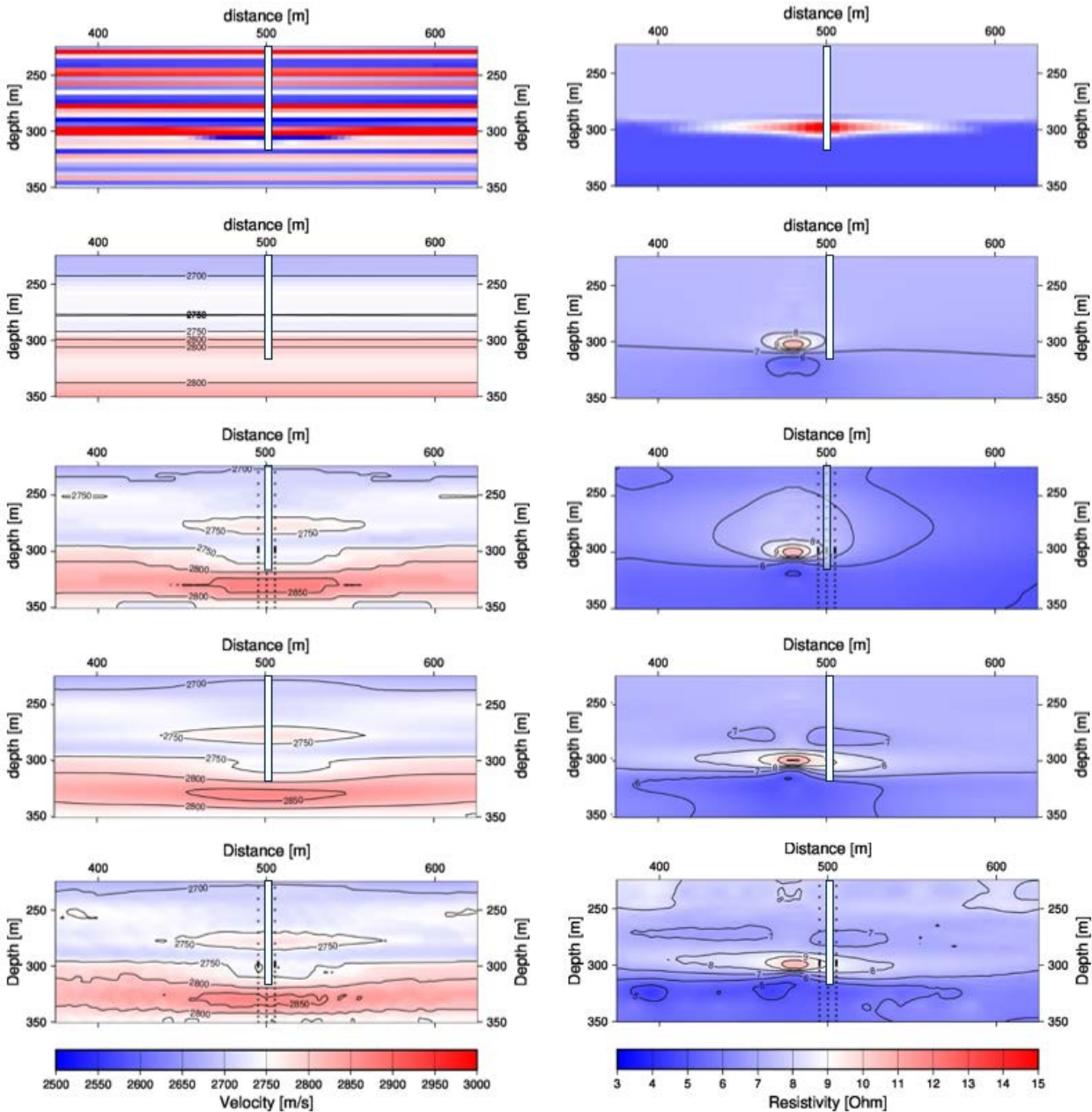


**Figure 6:** Comparison of joint inversion results for a three-layer petrophysical model defined at the well (495-505 m). The well location is indicated in white, the grid points of the petrophysical model are plotted as black crosses. Models in the left column are velocities, in the right column resistivities. The models are (top to bottom): "true models", starting models, petrophysical joint inversion results, structural joint inversion results, hybrid joint inversion results.

Figure 6 shows the comparison of joint inversion results for the three-layer petrophysical model defined at the well. The vertical extension of the petrophysical model is equal to the target area (225-350 m depth). The lateral extent of the model is 10 meters (495-505 m). Structural, petrophysical, and hybrid joint inversion results are displayed. While the resulting hybrid joint inversion models combine different features of the

structural and petrophysical ones, the main features of the hybrid result are similar to the ones in the structural one. The results show greatly reduced misfits of both structural and petrophysical constraints.

The hybrid joint inversion results show a clear improvement of the resolution of the CO<sub>2</sub> plume and surrounding structure, compared to independent inversions and individual joint inversion results. The petrophysics-based extension appears to provide valuable constraints, such as improved definition of the CO<sub>2</sub> plume and better separation between layers.

### 2.3.2 Joint inversion application to real FWI and ERT data from the Ketzin pilot site, Germany

Ketzin was Europe's longest-operating on-shore CO<sub>2</sub> storage facility (Martens et al., 2014), which successfully finished the complete storage site life cycle in 2018. Between June 2008 and August 2013, a total amount of 67 000 tonnes of CO<sub>2</sub> was injected and safely stored in a saline aquifer of the Upper Triassic Stuttgart Formation at depths between 630 m and 650 m. In August 2013, the CO<sub>2</sub> injection was completed, and the site abandonment was concluded in 2018 after several years of post-injection monitoring.

The joint inversion is applied to seismic data from 2012, after about 61 000 tonnes of CO<sub>2</sub> had been injected. Seismic FWI (3D) was applied to a line of receivers across the injection well and combined with the 2012 ERT surface downhole repeat survey, which was acquired a few months prior to the 2012 seismic repeat survey. The difference in the amount of injected CO<sub>2</sub> between these two surveys is about 1 000 tonnes.

The petrophysical model used in the application of the hybrid joint inversion to the Ketzin data was derived from a combination of well logs and laboratory measurements of rock samples. Three different lithological units were used for the petrophysical joint inversion (Figure 7): the Weser formation acting as overburden (589-634 m), the reservoir part of the Stuttgart formation (634-650 m), and the Stuttgart formation beneath the reservoir (650-710 m).

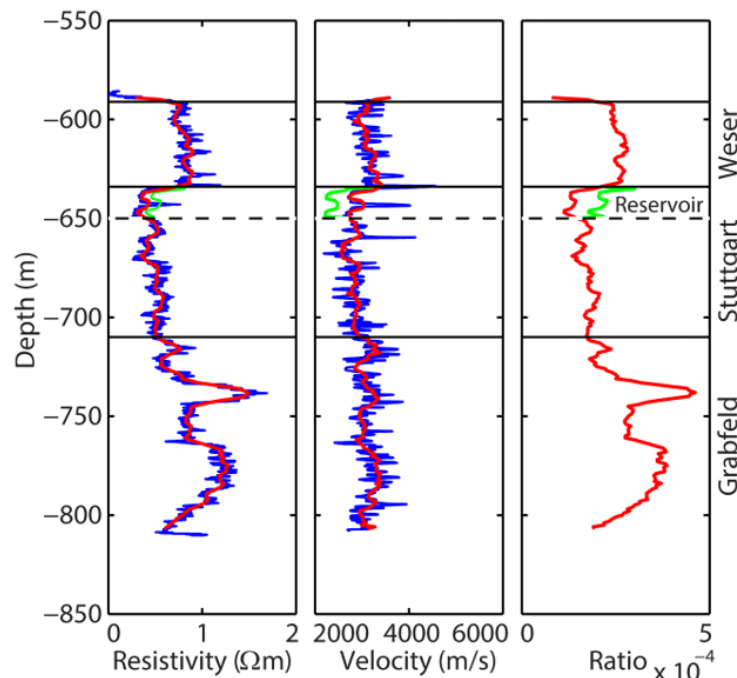


**Figure 7:** Results of the resistivity and sonic ( $V_p$ ) baseline logging from May 3, 2007 (blue). Logging results are interpolated at regular depth intervals of 1 m spacing, with a running average of 5 m applied (red). The effect of CO<sub>2</sub> replacing the pore fluid was derived from laboratory measurements for a CO<sub>2</sub> saturation of  $S_{CO_2} \approx 0.4$  (green). The transition between lithological units is indicated by the black lines.

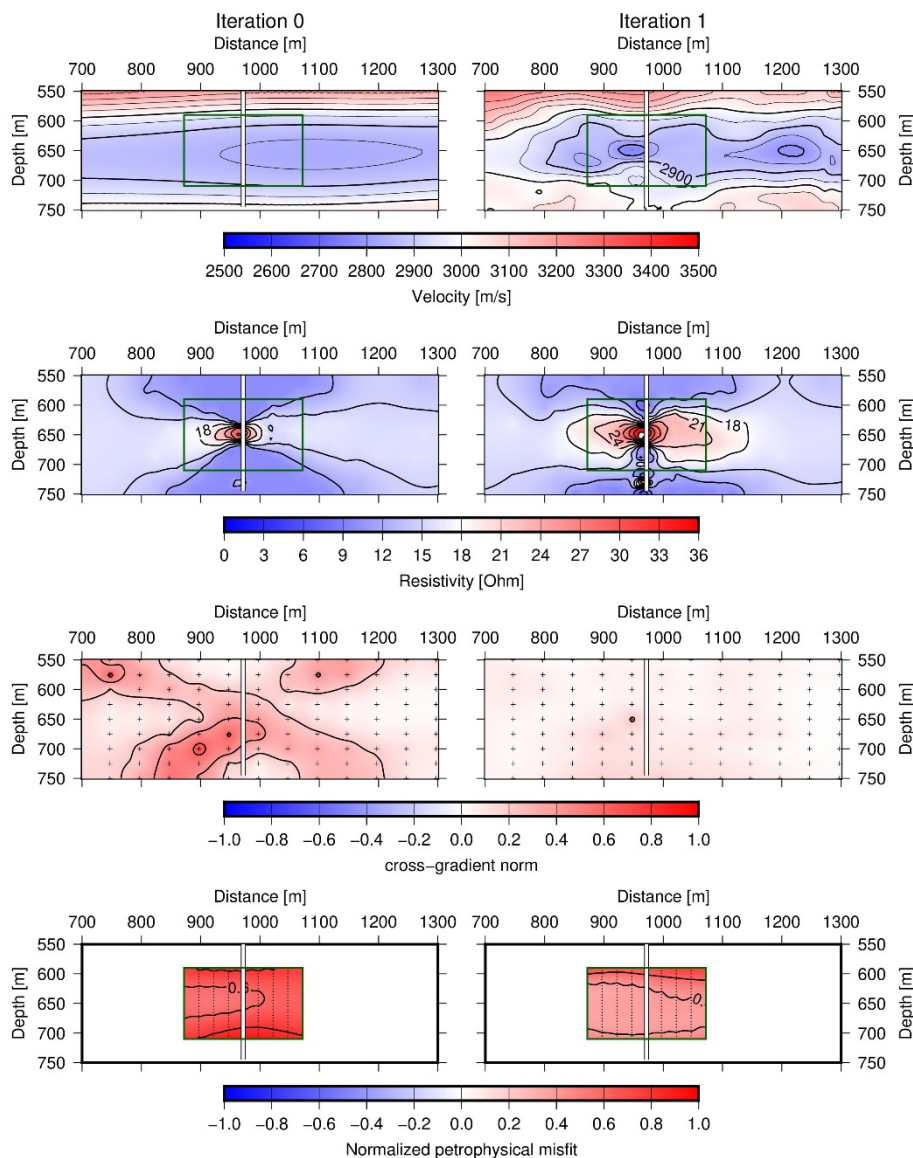


**Figure 8:** Hybrid joint inversion results for velocity models from FWI (top row), resistivity models from ERT (second row). Corresponding development of the cross-gradient vector and petrophysical constraint are shown in the third and fourth row, respectively. The left column refers to the starting models and the right one to the hybrid joint inversion results after one iteration. The extent of petrophysical models is indicated by green frames. The location of the monitoring well is shown as a white line.

Figure 8 shows an example of joint inversion results for the optimum parameters that were determined following the joint inversion workflow. Seismic and ERT starting models and results of the hybrid joint inversions are displayed after one iteration. In addition, the misfit reduction of structural and petrophysical constraints are plotted in the model space. In the case shown here, the petrophysical model extended 100 m from the monitoring well. It can be seen that misfits are reduced considerably in both cases. The aim for the data misfits during the joint inversion was to be the same or better than in the individual inversions. It could be shown that the hybrid joint inversion considerably improves the inversion result compared to individual or petrophysical joint inversion, but especially compared to the independent inversions.

### 2.3.3 Application to cross-well seismic and downhole ERT data from CaMI.FRS

The following section is an example of the application of the joint inversion code to 4D seismic cross-well and downhole ERT data from the Field Research Station (CaMI.FRS) in Canada. At CaMI.FRS CO<sub>2</sub> is injected in the water-filled Basal Belly River Sandstone (BBRS) Formation between a depth of 295 m and 305 m below ground surface (Macquet et al., 2019). Above the BBRS is the 152 m thick Foremost Formation, composed of clayey sandstone with interbedded coal layers, which provides a leaky cap-rock for the CO<sub>2</sub> storage complex (Lawton et al., 2017; Macquet et al., 2019).

Cross-well seismic baseline and monitor data were acquired by LBNL prior to the CO<sub>2</sub> injection and in December 2021, after almost 50 tonnes of CO<sub>2</sub> had been injected. Figure 9 shows an example of baseline and monitoring data. The monitoring data show strong attenuation around injection depth, most probably due to the presence of CO<sub>2</sub>, which made the 4D inversion in the affected depth range challenging. We chose travel-time tomography for imaging of the injected CO<sub>2</sub>. Repeatability of the seismic data is a prerequisite for accurate 4D inversion and interpretation. Hence the focus of the data processing was on accurate and consistent picks of the compressional wave arrivals for travel-time tomography.

Two ERT data sets from a 16-electrode downhole array in the CaMI.FRS geophysical observation well were selected for the 4D analysis: one acquired during the pre-injection phase in 2017, and one acquired in December 2021 at the same time as the cross-well seismic monitor survey.

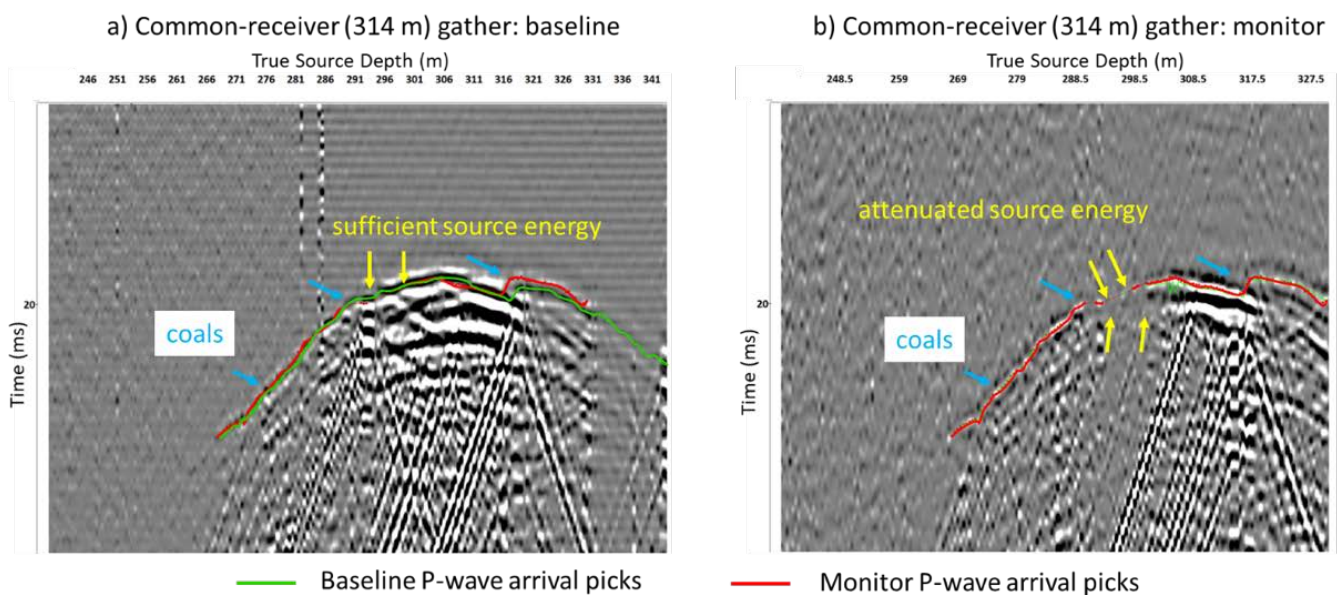


**Figure 9:** P-wave arrivals picks in common-receiver gathers at 314 m true vertical depth. The baseline data (a) have finer spatial sampling and higher signal-to-noise ratio compared with the monitor survey (b). In the target interval 290-300 m (yellow arrows) source energy get attenuated, likely by the CO<sub>2</sub> plume. Coal layers give rise to strong tube waves at 272 m, 290 m, and 316 m (cyan arrows).

In an attempt to cope with the challenging conditions due to the attenuation in the seismic data, we used an adapted optimized tomographic inversion scheme (Jordan, 2003; Smith et al., 2009). The inversion code allows arbitrary source and receiver positions and was originally developed for sparse or uneven ray distribution, using optimized model parameterization to cope with the lack of ray coverage as well as possible. For the inversion of the downhole ERT data we use the open-source "Boundless Electrical Resistivity Tomography" (BERT) algorithm for the ERT (Günther et al., 2006).

To investigate 4D changes in the subsurface due to the CO<sub>2</sub> injection, we perform two joint inversions, one for the 2017, and one for the 2021 seismic and ERT baseline and repeat data sets.

The seismic cross-well inversion was performed in several steps. In a first step, an initial velocity model was created based on a smoothed version of available well logs. In a second step, this initial velocity model was optimized so that all model parameters have a resolution value of at least 50% relative to the maximum resolution value in the model. This serves to ensure a stable seismic inversion and to avoid artefacts from the uneven ray distribution. In a third step, the optimized model was used as starting models for both baseline and repeat tomographic inversions.

Figure 10 shows the result of one iteration of the joint seismic-ERT inversions for baseline and repeat data sets. As the direct comparison of the baseline and monitor results are difficult, the corresponding difference plots are also provided.

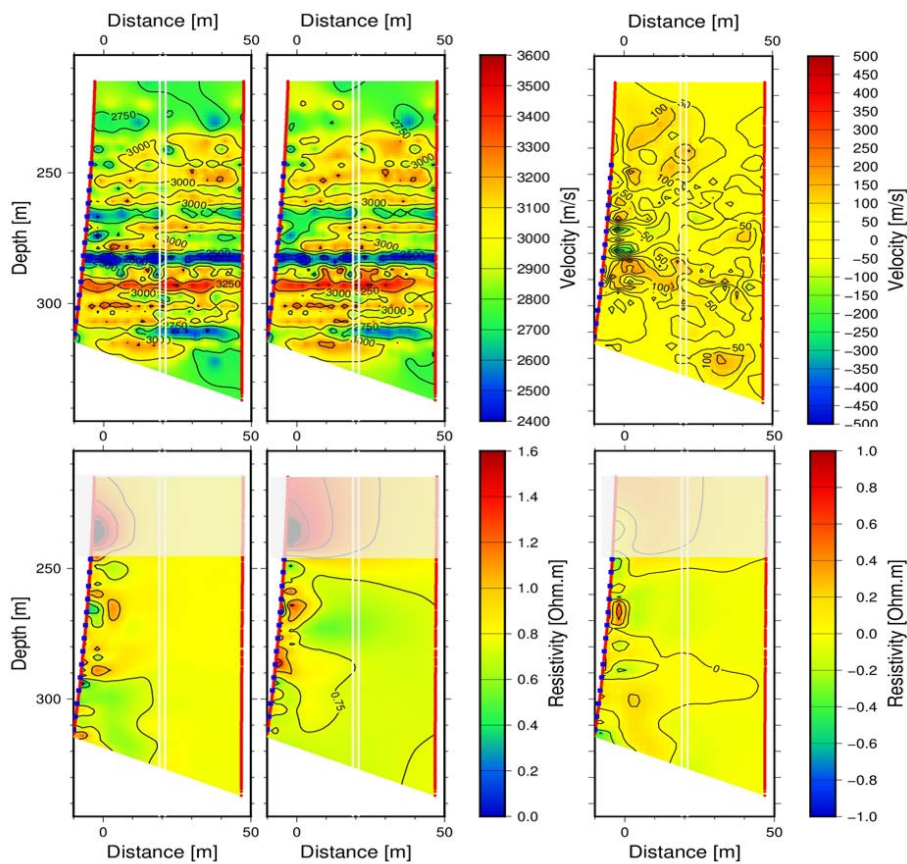


**Figure 10:** Joint inversion results for baseline (left) and repeat (middle) data sets and the 4D differences (right). Seismic velocity models are shown in the top row, resistivity models are shown in the bottom row. Observation wells and seismic sources and receivers are plotted in red, ERT electrodes in blue, and the injection well in white. The shaded area in the resistivity models indicates the depth range where no ERT electrodes exist.

The joint inversion results confirmed and improved the seismic result and allowed the ERT inversion to provide more insight away from the well. The joint inversion proved to behave very robustly, providing consistent results over a variety of different parameter settings. Lower velocities and higher resistivities can be interpreted as effects of potential presence of CO<sub>2</sub>. The results suggest that the CO<sub>2</sub> injected at CaMI.FRS migrates upwards from the injection depth. In addition, smaller low-velocity anomalies corresponding to

more diffuse increased resistivity values at the injection depth can most likely be attributed to the presence of CO<sub>2</sub>.

### 2.3.4 Application to VSP seismic and downhole ERT data from CaMI.FRS

This section shows the application of the joint inversion method to 4D seismic VSP and downhole ERT data from the Field Research Station (CaMI.FRS) in Canada. CO<sub>2</sub> is injected in the water-filled Basal Belly River Sandstone (BBRS) Formation between a depth of 295 m and 305 m below ground surface (Macquet et al., 2019).

The 4D vertical seismic profiling (VSP) seismic monitoring conducted in this study relies on travel-time tomography to image the subsurface changes caused by the CO<sub>2</sub> injection. We inverted the arrival times of the seismic waves propagating between the shot points at the surface, as indicated in Figure 11, and the receivers in the observation borehole. These are installed permanently outside the well casing at depths between 190-305 m below the surface. Data were acquired in May 2017, before any CO<sub>2</sub> was injected, and in March 2022, with about 50 tonnes of CO<sub>2</sub> in the ground. The line of shot points for the VSP survey used in this study and the position of wells at CaMI.FRS are shown in Figure 2. The geophysical monitoring well (Obs2), located 20 m south-west from the injection well hosts the borehole geophone array, which is composed of 24 3-component geophones at intervals of 5 m. The source used for the VSP survey was the University of Calgary's IVI Envirovibe, which used a 10-150 Hz sweep over 16 seconds. Shot spacing was 10 m.

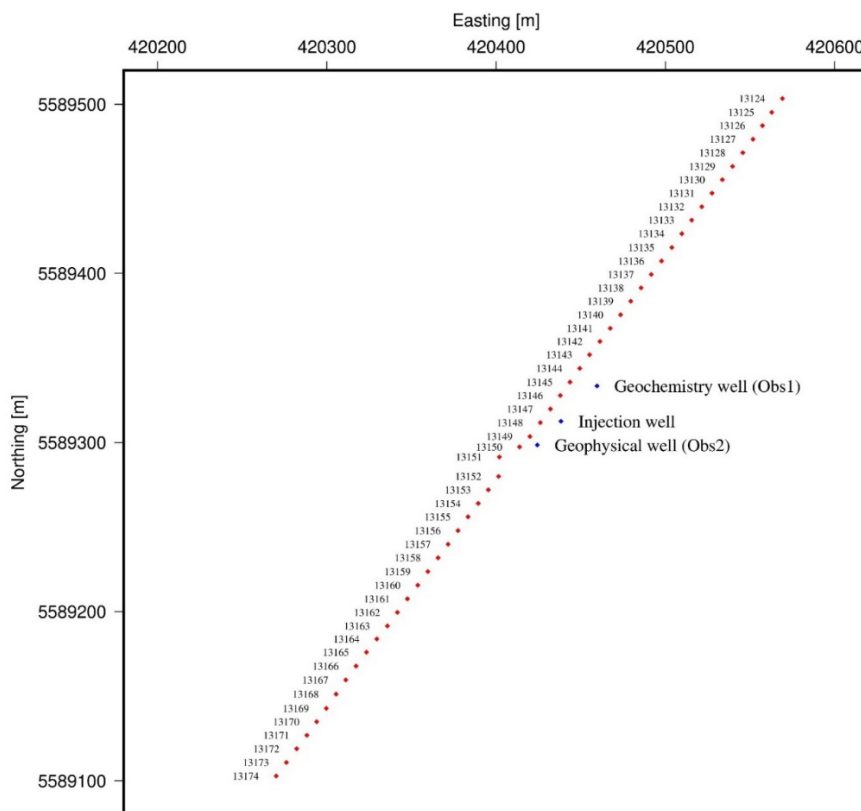


**Figure 11:** Map of vibroseis shot points 13124 to 13174 and injection well, geophysical observation well (Obs2), and geochemistry well (Obs1) at the CaMI.FRS site. The receivers are located in the geophysical observation well.

First arrival time picks were extracted from the vertical component of the waveform data with focus on suitability for 4D analysis. Unfortunately, several receivers in the lower part of the monitoring well were either dead or strongly affected by noise and had to be removed (285 m and 290 m) or interpolated (300

m). This posed an especially difficult situation for the seismic inversion, as the injection point is around 300 m deep and outside the ray coverage of the first arrival time data.

During the initial 4D analysis of the travel time data, significant, systematic travel time offset between shots from baseline and monitor data sets could be observed. This was interpreted as effects of changes of the shallow surface conditions (e.g., potential freezing) in baseline and monitoring surveys, and the offsets were corrected for each shot pair by aligning the travel times observed at the uppermost receiver recordings between 190 m and 250 m. These were most consistent in the travel time plots and are also expected to be least affected by 4D changes due to the CO<sub>2</sub> injection.

The corresponding 4D ERT data were acquired during 2017, prior to the CO<sub>2</sub> injection and in December 2021 when almost 51 t of CO<sub>2</sub> were injected. The downhole electrodes are spaced every 5 m and located between ~245-320 m below ground level.

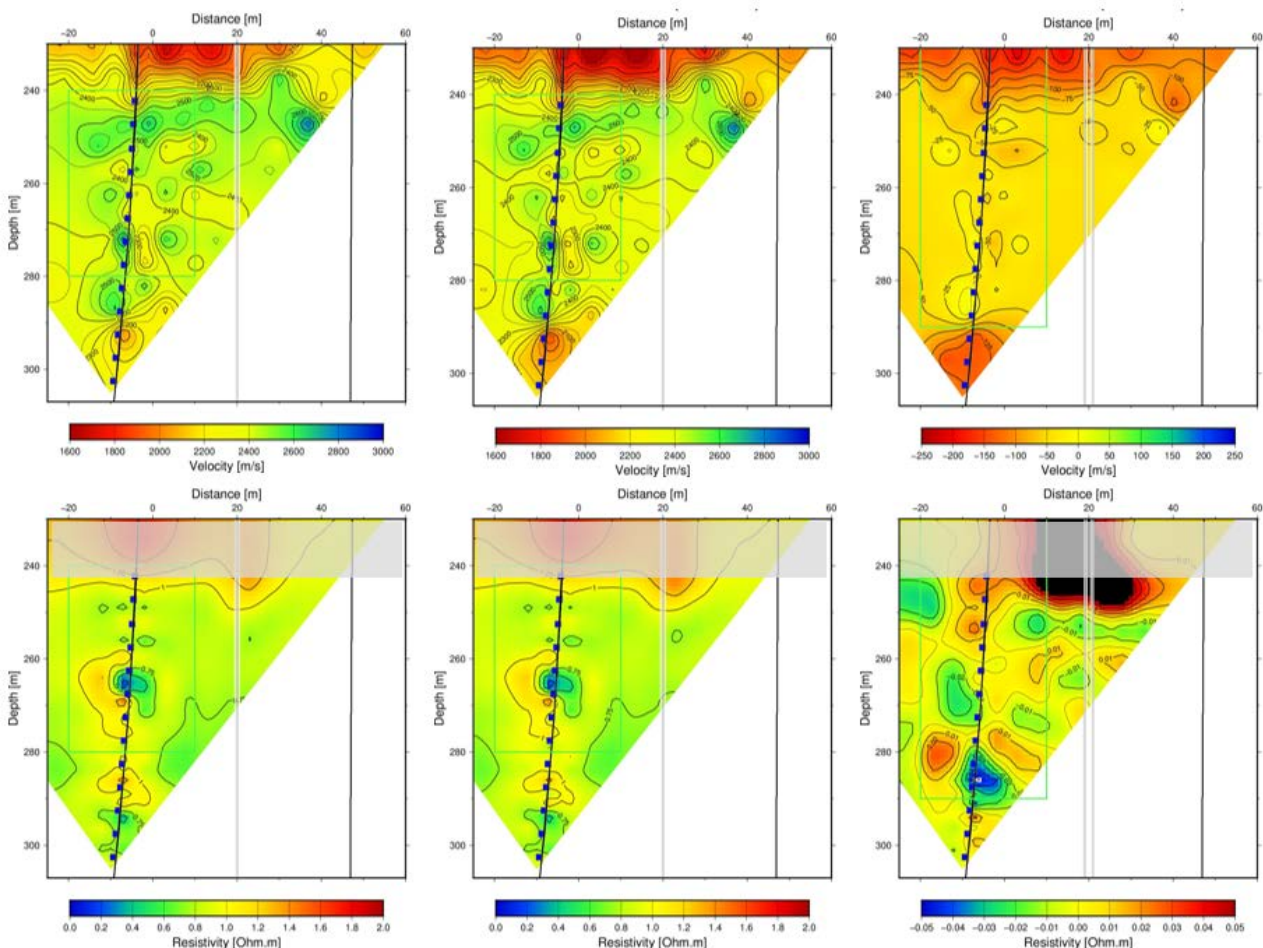


**Figure 12:** Joint inversion results for baseline(left) and repeat (middle) data sets and the 4D differences (right). Seismic velocity models are shown in the top row, resistivity models are shown in the bottom row. Observation wells and are plotted in black, ERT electrodes in blue, and the injection well in white. The shaded area in the resistivity models indicates the depth range where no ERT electrodes exist.

The seismic VSP and ERT downhole data are inverted using the same optimized tomographic and ERT inversion schemes as described in section 2.3.3.

Joint inversion results are shown in Figure 12 after one iteration of joint seismic-ERT inversion for baseline and repeat data sets, and the difference between them. The area of the resistivity models where no ERT electrodes exist is shaded.

The inversion was challenging as the geometry of the VSP seismic first arrival time data only illuminated a very narrow region around the observation well, about 20 m from the injection point. In addition, two sensors at 285 m and 290 m depth were not available, resulting in only few data to illuminate the injection depth and to observe any potential effects from the injected CO<sub>2</sub> in the injection horizon. The ray geometry resulted in a rather limited area around the geophysical observation well, where the joint inversion could be applied. The maximum depth was limited to 290 m, which was above the injection depth. In our analysis we focus on the lower depth range between 240 m and 310 m where both seismic receivers and ERT electrodes exist. The joint inversion appears to act more on seismic model than on the ERT one, potentially because the seismic model is not well constrained at depth. Main common 4D features in velocity and resistivity models are reduced seismic velocities and increased resistivities at around 300m depth, between 250 and 260m to the left of the observation well, and at around 250m around and to the left of the injection well. These may be related to the presence of CO<sub>2</sub>.

In all tested cases the joint inversion was able to improve the joint inversion misfit while maintaining or improving the misfit of the individual data sets, compared to independent seismic and ERT inversions. The joint inversion acts as powerful data-driven regularization on the inversion that can help identifying common structures. This worked even under difficult conditions and for challenging geometries, where the 4D challenge may have been larger than the one applying the joint inversion.

## 2.4 Petrophysical quantification and interpretation

To demonstrate the second step of the 2-step quantification of key reservoir parameters described in section 2.2.1, we applied a SINTEF in-house rock-physics inversion tool to joint inversion results from the cross-well seismic and ERT data described in section 2.3.3.

As input for the rock physics inversion, velocity and resistivity profiles were extracted along the geophysical observation well at CaMI.FRS. Thanks to a Bayesian formulation, we can incorporate prior information and assess uncertainties. In our approach, we use the neighborhood algorithm (NA) following the work of Dupuy et al. (2021). The Bayesian inversion is done in two steps: (1) a search stage aiming at exploring the model space and deriving misfit/probability density for each model, and (2) an appraisal or sampling stage taking the results of the first step and resampling them to derive a statistically consistent probability distribution. Using Biot-Gassmann (for seismic) and Archie (for ERT) rock physics models results in a set of 14 parameters that must be estimated to derive P-wave velocity and resistivity. The porosity was directly given by log data. The grain properties were estimated using the Hill average (Hill, 1952) of quartz, illite, coal, and carbonate volume fractions. The dry bulk and shear moduli were estimated using Gassmann equations from sonic P and S-wave velocities. These parameters could also be estimated with uncertainty using Bayesian rock physics inversion from baseline seismic and ERT data (Dupuy et al., 2021).

Figure 13 provides the 1D profiles of P-wave velocity and bulk resistivity estimated by seismic and ERT joint inversion and used as input data in the rock physics inversion at the observation well between 250 and 305 m depth. In the Bayesian rock physics inversion, we assume the velocity model is known with 5% error and resistivity model with 20% error.

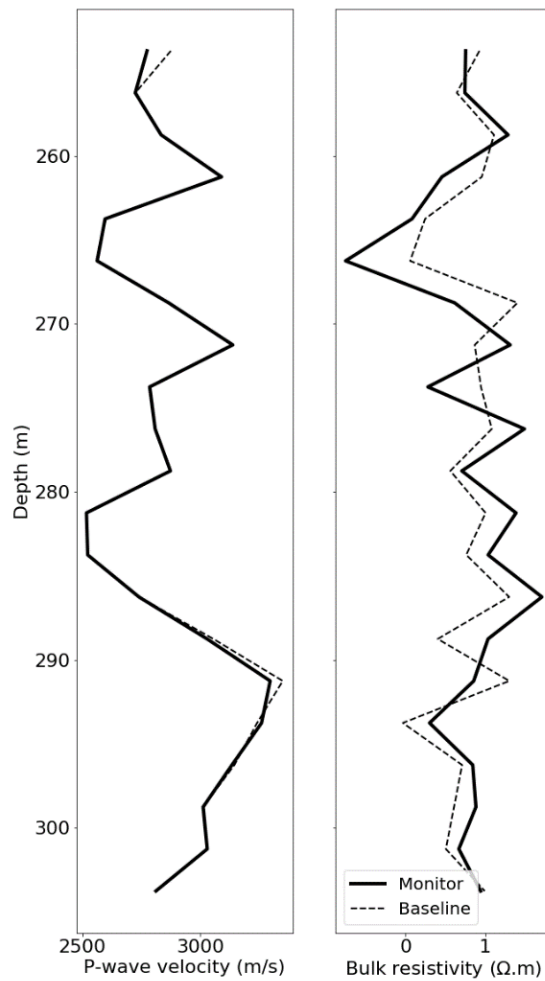


**Figure 13:** 1D profile of P-wave velocity and bulk resistivity at the observation well. The continuous lines indicate the monitor models while the dashed lines represent the baseline models.

We used the input given in Figure 13 (i.e., P-wave velocity and resistivity) for the monitor case to invert for CO<sub>2</sub> saturation and patchiness exponent. The other parameters in the rock physics model were assumed to be known and constant and are not updated by the inversion. The CO<sub>2</sub> saturation models can take values between 0 and 1 and the patchiness exponent models can have values between 1 and 40 (patchy and uniform mixing, respectively).

Figure 14 shows the resulting full 1D profiles at the observation well for the CO<sub>2</sub> saturation and patchiness exponent. The plots provide the confidence intervals and mean value for each parameter.

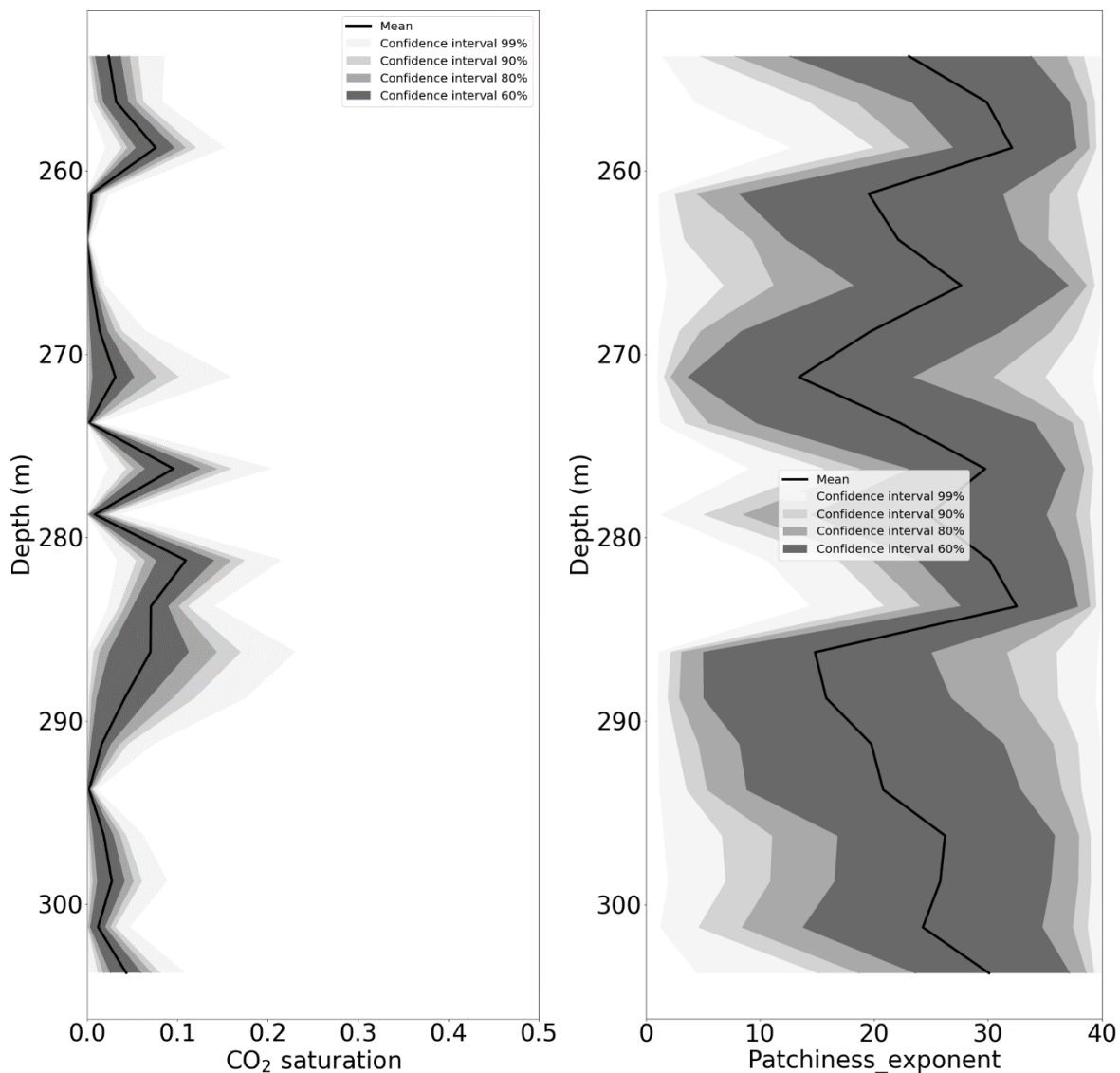


**Figure 14:** CO<sub>2</sub> saturation and patchiness exponent profiles at the observation well. The estimates are given through confidence intervals and mean values. The plots are providing the confidence intervals and mean value for each parameter. The input data are P-wave velocity and bulk resistivity derived by joint inversion and given in Figure 13.

The rock physics inversion results (Figure 14) show several zones where non-zero CO<sub>2</sub> saturation is observed around the geophysical observation well, about 20 m from the injection well. These are consistent with previous observations and the geology derived from logs (Macquet, pers. comm.). The results show a CO<sub>2</sub> saturation of 3% just above 300 m, which corresponds to the injection depth and the Basal Belly River Sand Stone. In addition, two larger zones with up to ~10% of CO<sub>2</sub> saturation can be identified around 280 m depth. These correspond to coal layers. In addition, a fourth zone with a minor CO<sub>2</sub> saturation of up to 3% is found that corresponds to sandstone (aquifer) between 269 and 273 m depth. However, as the rock physics model used here was designed for sandstone areas where different rock types are present, this cannot be interpreted quantitatively.

## 2.5 Tilt measurements and derivation of strain

The feasibility study for monitoring of CO<sub>2</sub> injection at the CaMI.FRS site was documented in deliverable L1. The results of this study are summarized in this section.

The expected surface deformation was modelled for the CaMI.FRS site based on the expected injection rates at the beginning of the project, accumulating to more than 1700 t after 5 years of injection. Figures 15 and 16 show the modelled reservoir expansion surface uplift after 1 and 5 years of injection.

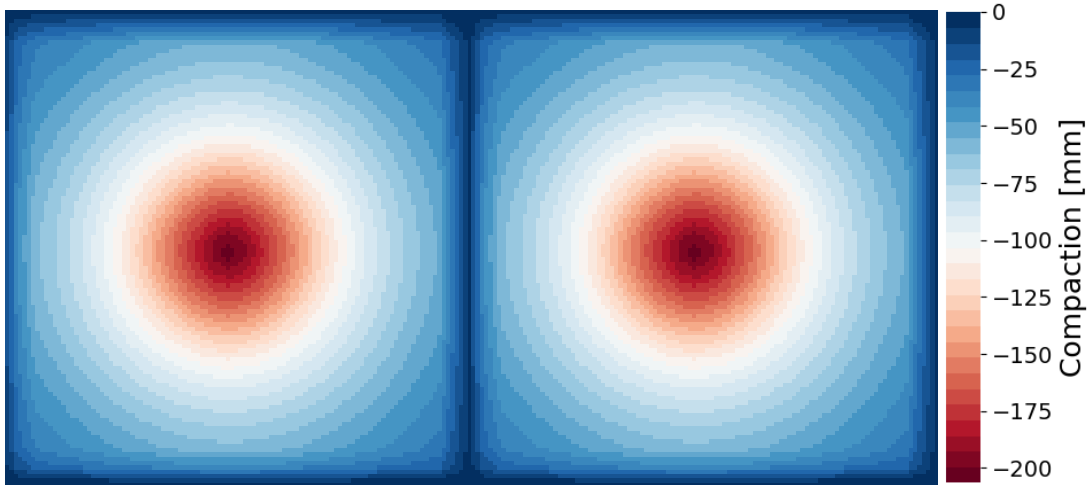


**Figure 15:** Reservoir expansion in a 500 m x 500 m model, in map view. Left: After 1 year, right: after 5 years.

The maximum expansion is about 200 mm after 5 years, in a small area around the injection point.

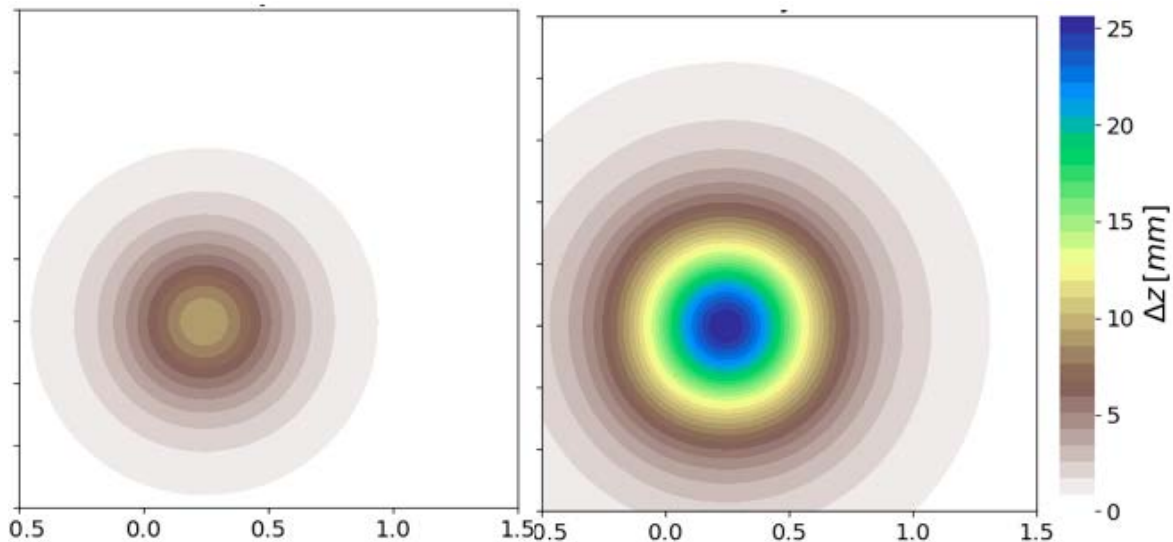


**Figure 16:** Modelled surface uplift in map view after 1 year (left) and 5 years (right). The model is 2 km x 2 km.

Surface uplift of a maximum of about 9 mm after 1 year and 25 mm after 5 years of injection was modelled (Figure 16) based on the supplied flow model and pore compressibility of  $4.18 \cdot 10^{-4} \text{ bar}^{-1}$ . This may be just above the detection level for monitoring vertical movements.

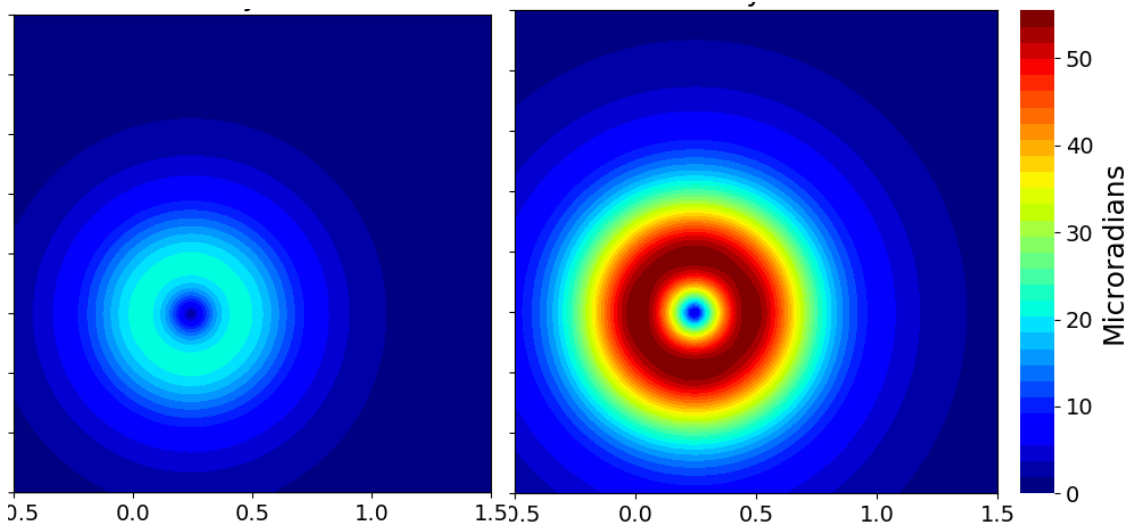


**Figure 17:** Surface tilt change since injection start, in map view. Left: after 1 year. Right: after 5 years. The dimension of the model is 2 km x 2 km.

A maximum tilt change is estimated at about 20  $\mu$ Rad after 1 year and 50  $\mu$ Rad after 5 years. This is well above the instrumental noise levels (by a factor of 1000) of a tiltmeter.

Given the originally planned injection rate, our conclusion was that it may be feasible to monitor such tilt changes with commercially available instruments. However, it was proposed to install a tiltmeter under development at UCSD, with potentially higher resolution and better drift stability. A test installation of two tiltmeters, about 250 m and 500 m away from the injection point was recommended.

Site independent, the outcome of the modelling showed clearly that if surface deformation is considered as an additional monitoring method for CO<sub>2</sub> storage sites, the application of tilt meters may be beneficial if the expected surface deformation is small.

### 3 Meetings, reports, presentations, and publications

#### Main meetings:

- 28.08.2017: Kick-off meeting
- 17.01.2018: Status meeting
- 26.06.2018: Status meeting
- 29.01.2019: Status meeting and separate steering (SC) committee meeting
- 22.08.2019: Status meeting (during FRS meeting in Calgary; no separate SC meeting)
- 08.06.2020: Status meeting and separate SC meeting
- 19.01.2021: Status meeting and separate SC meeting
- 03.06.2021: Status meeting and separate SC meeting
- 24.11.2021: only SC meeting
- 28.04.2022: Status meeting and separate SC meeting

Technical meetings were conducted when needed.

#### Reports:

Ten reports were created and provided as deliverables L1-L9 as already mentioned in section 1.

- L1 Tilt meter feasibility study Feasibility of tiltmeter monitoring of CO<sub>2</sub> injection at the FRS site
- L2 CaMI.FRS baseline program: Overview of baseline measurements, data processing and existing models for the different geophysical monitoring techniques
- L3 CaMI.FRS geophysical monitoring program: Overview of the CaMI.FRS geophysical monitoring program, including baseline and repeat measurements, data processing and existing models for the different geophysical monitoring techniques
- L4 Emerging monitoring methods for large-scale CO<sub>2</sub> storage: Overview of emerging monitoring methods relevant for joint inversion and quantitative CO<sub>2</sub> monitoring
- L5 Joint inversion code v1.0: Status of the first version of the joint inversion method and implementation
- L6a Hybrid structural-petrophysical joint inversion (version 2.0)
- L6b Hybrid structural petrophysical joint inversion as a novel inversion technique: Application to CO<sub>2</sub> monitoring at the Ketzin pilot site: Manuscript for publication about validation of the joint inversion code with real data focusing on the joint inversion
- L7 Joint inversion of cross-well seismic and ERT at the Field Research Station, Canada: Manuscript for publication about demonstration of code for first scenario/data set
- L8 CO<sub>2</sub> monitoring using joint inversion of VSP seismic and ERT data at the Field Research Station, Canada: Manuscript for publication about demonstration of code for second scenario/data set
- L9 Quantification of CO<sub>2</sub> saturation at CaMI.FRS: Report

## Publications:

- **Presentations:**

**Rippe, D., Strom, A., Schmidt-Hattenberger, C., Jordan, M., Lawton, D., Saeedfar A. (2017)**, Electrical resistivity tomography for CO<sub>2</sub> migration monitoring at the Field Research Station near Brooks, AB (Canada), Annual meeting of the German Geophysical Society, March 27.–30., Potsdam, Germany

**Jordan, M., Rippe, D., Schmidt-Hattenberger, C., & Romdhane, A. (2017)**. Joint Inversion for Improved CO<sub>2</sub> Monitoring at the Ketzin Pilot Site, Germany. In *EAGE/SEG Research Workshop 2017* (pp. cp-522). European Association of Geoscientists & Engineers.

**Jordan, M., Rippe, D., Romdhane, A., & Schmidt-Hattenberger, C. (2018)**. CO<sub>2</sub> monitoring at the Ketzin pilot site with joint inversion: Application to synthetic and real data. In *Fifth CO<sub>2</sub> Geological Storage Workshop* (Vol. 2018, No. 1, pp. 1-5). European Association of Geoscientists & Engineers.

**Rippe, D., Jordan, M., Romdhane, A., Schmidt-Hattenberger, C., Macquet, M., & Lawton, D. (2018)**. Accurate CO<sub>2</sub> monitoring using quantitative joint inversion at the CaMI Field Research Station (FRS), Canada. In *14th International Conference on Greenhouse Gas Control Technologies-GHGT-14*.

**Jordan, M., Rippe, D., Romdhane, A., Macquet, M., & Lawton, D. C. (2019)**. CO<sub>2</sub> Monitoring Using Hybrid Structural-Petrophysical Joint Inversion at the CaMI Field Research Station (CaMI. FRS), Canada. *AGU Fall Meeting, 2019*, S31E-0566.

**Jordan, M., Rippe, D., aCQurate project team (2019)**. Joint inversion for quantitative imaging of reservoir parameters and ERT data acquisition at CaMI.FRS. IEAGHG Monitoring Network and Environmental Research Network Workshops 2019, Calgary, AB, Canada, 19-23 Aug 2019.

**Jordan, M., Rippe, D., Romdhane, A., Schmidt-Hattenberger, C., Lawton, D., Macquet, M. (2019)**. Joint inversion of synthetic monitoring data for a realistic model from CaMI Field Research Station (FRS), Canada. 10th International Trondheim CCS Conference-TCCS-10, Trondheim, Norway, 17-19 Jul 2019.

**Rippe, D., Jordan, M., Schmidt-Hattenberger, C., Lawton, D., Macquet, M. (2019)**. Monitoring activities at the CaMI Field Research Station in Brooks, AB, Canada. 2nd Pre-ACT Stakeholder Workshop. Mission: Safe and cost-effective CO<sub>2</sub> storage for European Industries. Brussels, Belgium, 10 Oct 2019.

**Jordan, M., Rippe, D., Romdhane, A., Macquet, M., Lawton, D. (2019)**. CO<sub>2</sub> Monitoring Using Hybrid Structural-Petrophysical Joint Inversion at the CaMI Field Research Station (CaMI.FRS), Canada. 2019 Fall Meeting, AGU, San Francisco, CA, USA, 9-13 Dec 2019. S31E-0566.

**Jordan, M., Rippe, D., Romdhane, A., Macquet, M., & Lawton, D. C. (2019)**. CO<sub>2</sub> Monitoring Using Hybrid Structural-Petrophysical Joint Inversion at the CaMI Field Research Station (CaMI. FRS), Canada. *AGUFM, 2019*, S31E-0566.

**Rippe, D., Jordan, M., Macquet, M., Lawton, D., Romdhane, A., & Eliasson, P. (2020)**. Quantitative CO<sub>2</sub> monitoring at the CaMI Field Research Station (CaMI. FRS), Canada, using a hybrid structural-petrophysical joint inversion. In *EGU General Assembly Conference Abstracts* (p. 8163).

**Jordan, M., Rippe, D., Romdhane, A., Eliasson, P., Dupuy, B., Macquet, M., Lawton, D. (2020)**. Towards quantitative CO<sub>2</sub> monitoring using hybrid joint inversion. SEG Postconvention Workshop, Society of Exploration Geophysicists

**Rippe, D., Jordan, M., Romdhane, A., Schmidt-Hattenberger, C., Macquet, M., & Lawton, D. (2020)**. Hybrid structural-petrophysical joint inversion for CO<sub>2</sub> monitoring-examples from Ketzin and CaMI. FRS CO<sub>2</sub> pilot sites. In *AGU Fall Meeting Abstracts* (Vol. 2020, pp. S009-0002).

**Jordan, M., Rippe, D., Anouar, R., Eliasson, P., & Schmidt-Hattenberger, C. (2022)**. Hybrid Structural Petrophysical Joint Inversion as a Novel Inversion Technique for CO<sub>2</sub> Monitoring. In *EAGE GeoTech 2022 Sixth EAGE Workshop on CO<sub>2</sub> Geological Storage* (Vol. 2022, No. 1, pp. 1-5). European Association of Geoscientists & Engineers.

**Jordan, M., Rippe, D., Romdhane, A., Eliasson, P., Dupuy, B., Macquet, M., Lawton, D. (2020)**. Towards quantitative CO<sub>2</sub> monitoring using hybrid joint inversion. SEG Postconvention Workshop, Society of Exploration Geophysicists

- **Papers:**

**Rippe, D., Jordan, M., Romdhane, A., Eliasson, P., and Schmidt-Hattenberger, C.** Hybrid structural petrophysical joint inversion as a novel inversion technique: Application to CO<sub>2</sub> monitoring at the Ketzin pilot site, prepared for publication in Geophysical Journal International

**Jordan, M., Alumbaugh, D., Glubokovskikh, S., Macquet, M., Rippe, D.** Joint inversion of cross-well seismic and ERT at the Field Research Station, Canada; Jordan, M., Alumbaugh, D., Glubokovskikh, S., Macquet, M., Rippe, D., in preparation for IJGHG

**Jordan, M., Pavez-Orrego, C., Macquet, M., Kolkman-Quinn, B., Rippe, D.** CO<sub>2</sub> monitoring using joint inversion of VSP seismic and ERT data at the Field Research Station, Canada, in preparation for IJGHG

- **Webinars:**

**Jordan, M. (2021).** CO<sub>2</sub> monitoring using hybrid structural-petrophysical joint inversion. presentation in NCCS webinar series, <https://www.sintef.no/projectweb/nccs/webinars/>

- **Invited presentation:**

**Jordan, M., Rippe, D., Romdhane, A., Eliasson, P., (2022).** Hybrid structural-petrophysical joint inversion of different geophysical data types for improved reservoir monitoring. Multiple Approaches to Time-Lapse Monitoring for Carbonate Reservoirs Workshop. SEG Workshop, Abu Dhabi, May, 24th-26th.

- **Other publications and presentations:**

Project presentations at **CLIMIT SUMMIT** (2017, 2019, 2021)

**Article** about aCQurate project: aCQurate project developing integrated CO<sub>2</sub> storage monitoring, Mark Lowey (2017), Carbon Capture Journal, Nov/Dec 2017, Issue 60

## 4 Project implementation and resource use

A joint SINTEF-GFZ postdoc, located at GFZ, was working tightly with SINTEF, CaMI, and LBNL on the implementation of the joint inversion method, ERT measurements and data processing, and joint inversion testing and application. The postdoc was working in constant contact with SINTEF.

A strong collaboration with Canadian, US, and German partners was established, with frequent contact to discuss data processing, inversions, and interpretation, comparison of results:

- M. Jordan visited LBNL, in December 2019 to discuss technical details regarding the cross-well measurements, and the implementation of the cross-well methods in the joint inversion.
- Several visits of CaMI and the University of Calgary to project meetings were conducted, including visits at the CaMI.FRS site, as well as visits of the North American partners to SINTEF.
- A Phd student from University of Calgary (Scott Keating) visited SINTEF in Fall 2018 for three weeks. A later longer visit was planned but could not be realized due to the Covid pandemic.

Additional collaboration was established with Columbia University (Kerry Key) using their Mare2DEM code, which then was also included in the aCQurate joint inversion code.

The project was awarded in October 2016 and the final contract was signed in May 2017. While the project end was originally planned in June 2020, the project was considerably delayed for a number of reasons:

- A failure of topside injection equipment (pump) in occurred in 2019, which caused a two-month delay.
- On-site computers that steered the injection and allowed communication with and remote control of the site were hacked, which caused an additional delay of almost two months.
- The injectivity at CaMI.FRS was lower than anticipated so that the detection threshold was reached significantly later than originally predicted. CO<sub>2</sub> could be first clearly detected from surface based seismic in the March '21 VSP survey.
- The Covid 19 pandemic severely impeded the field work, due to travel restrictions and restrictions for conduction field work within Canada. In the case of the field work conducted by LBNL, this meant that the US – Canada border was closed for about 18 months to all non-essential visitors due to COVID19 until September 2021. Final monitor measurements were conducted as late as December 2021 and January 2022, due to additional travel restrictions imposed by USDOE on the US national labs, and challenges for transporting the necessary equipment from the US to the CaMI.FRS site in Canada due to shortage of truck transportation in North America.
- SINTEF experienced some resource problems in the geophysics group. To solve this problem, in 2019 SINTEF hired a person that was living in the US at the time, and that was supposed to start in early 2020 at SINTEF in Norway. Due to the Covid pandemic this person could neither obtain a visa to Norway nor travel. This led to a series of delays of the start date before the person decided not to come to at all. This was ameliorated partially by extending the Postdoc position but could not completely avoid delays in the project.

As real data from CaMI.FRS that contained CO<sub>2</sub> effects were delayed, the initial validation of the code with real data was conducted using data from the Ketzin pilot site in Germany.

To demonstrate the code with real data using two scenarios from the CaMI.FRS site it had been originally planned to conduct a joint cross-well seismic and cross-well CSEM inversion and a joint VSP seismic and downhole ERT inversion. In preparation for this, in 2020 and 2021 joint inversions of cross-well seismic and cross-well CSEM data were conducted for the baseline data. Analogously, VSP seismic and downhole ERT baseline data also were jointly inverted to prepare for the joint inversion of the monitor data.

The cross-well seismic and CSEM inversions were conducted in collaboration with LBNL, wo did the acquisition and pre-processing of the seismic data as well as the picking of the seismic arrival times. The ERT

inversions were conducted in collaboration with CaMI and GFZ. The CSEM inversion was performed by LBNL and Columbia University (Kerry Key).

When the seismic cross-well data from the monitor survey were analyzed by LBNL it was observed that most of the seismic energy in the injection horizon was attenuated heavily by the injected CO<sub>2</sub> so that almost no direct arrival time picks could be extracted from this depth interval for the monitor data set. The two data sets were made comparable in a 4D sense by LBNL, and the seismic inversion was optimized so that a 4D result could be obtained, and so that the data could be used in a joint inversion and used to analyze changes in the subsurface due to the CO<sub>2</sub> injection.

For the planned VSP-CSEM joint inversion, the December 2021 cross-well repeat CSEM data acquisition suffered technical problems so that the data were not comparable to the baseline ones. Therefore, it was decided to conduct a joint inversion of VSP seismic and downhole ERT data instead.

The main difficulties that were observed in the application of the method to real data were not from the joint inversion itself, but rather from the 4D repeatability of the data.

## 5 References

Dupuy, B., Romdhane, A., Nordmann, P., Eliasson, P., and Park, J., Bayesian rock-physics inversion: Application to CO<sub>2</sub> storage monitoring, *GEOPHYSICS* 2021 86:4, M101-M122

Gallardo, L.A., Meju, M.A. (2004). Joint two-dimensional dc resistivity and seismic travel time inversion with cross-gradients constraints. *Journal of Geophysical Research: Solid Earth*, 109(B3), B03311.

Gassmann, F., 1951, Über die elastizität poröser medien: Vierteljahrsschrift der Naturforschenden Gesellschaft in Zurich, 96, 1–23.

Günther, T., Rücker, C., Spitzer, K. (2006). Three-dimensional modelling and inversion of dc resistivity data incorporating topography: ii. inversion. *Geophysical Journal International*, 166(2), 506–517.

Hill, R. 1952. The elastic behavior of a crystalline aggregate. *Proceedings of the Physical Society Section A*, 65, 349–354, <https://doi.org/10.1088/0370-1298/65/5/307>

Jordan, M., Rippe, D., Romdhane, A., & Schmidt-Hattenberger, C. (2018, November). CO<sub>2</sub> monitoring at the Ketzin pilot site with joint inversion: Application to synthetic and real data. In *Fifth CO<sub>2</sub> Geological Storage Workshop* (Vol. 2018, No. 1, pp. 1-5). European Association of Geoscientists & Engineers.

Key, K. (2016). MARE2DEM: a 2-D inversion code for controlled-source electromagnetic and magnetotelluric data. *Geophysical Journal International*, 207(1), 571-588.

Lawton, D., Bertram, M, Saeedfar, A., Macquet, M., Hall, K., Bertram, K., Innanen, K., Isaac, H. (2017). DAS and seismic installations at the CaMI Field Research Station, Newell County, Alberta. *CREWES Research Report — Volume 29* (2017).

Macquet, M., Lawton, D., Saeedfar, A., Osadetz, K.; A feasibility study for detection thresholds of CO<sub>2</sub> at shallow depths at the CaMI Field Research Station, Newell County, Alberta, Canada. *Petroleum Geoscience* 2019;; 25 (4): 509–518. doi: <https://doi.org/10.1144/petgeo2018-135>

Smith, R. B., Jordan, M., Steinberger, B., Puskas, C. M., Farrell, J., Waite, G. P., ... & O'Connell, R. (2009). Geodynamics of the Yellowstone hotspot and mantle plume: Seismic and GPS imaging, kinematics, and mantle flow. *Journal of Volcanology and Geothermal Research*, 188(1-3), 26-56.



Tarantola, Albert. Inverse problem theory and methods for model parameter estimation. Vol. 89. siam, 2005.

Martens, S., Möller, F., Streibel, M., Liebscher, A., The Ketzin Group (2014). Completion of five years of safe CO<sub>2</sub> injection and transition to the post-closure phase at the Ketzin pilot site. Energy Procedia, 59, 190–197.

Zeyen, H., & Achauer, U. (1997). Joint inversion of teleseismic delay times and gravity anomaly data for regional structures. In Upper mantle heterogeneities from active and passive seismology (pp. 155-168). Springer, Dordrecht.